DNA damage–induced p53 downregulates expression of RAG1 through a negative feedback loop involving miR-34a and FOXP1

Received for publication, March 11, 2024, and in revised form, October 15, 2024 Published, Papers in Press, October 23, 2024,
https://doi.org/10.1016/j.jbc.2024.107922

Katarina Ochodnicka-Mackovicova[1,2], Martine van Keimpema[1,2], Marcel Spaargaren[1,2,3], Carel J. M. van Noesel[1,2], and Jeroen E. J. Guikema[1,2,*]

From the [1]Department of Pathology, Amsterdam University Medical Centers, Location AMC, University of Amsterdam, Amsterdam, The Netherlands; [2]Lymphoma and Myeloma Center Amsterdam (LYMMCARE), Amsterdam, The Netherlands; [3]Cancer Center Amsterdam (CCA), Cancer Biology and Immunology - Target & Therapy Discovery, Amsterdam, The Netherlands

Reviewed by members of the JBC Editorial Board. Edited by Patrick Sung

During the maturation of pre-B cells, the recombination activating gene 1 and 2 (RAG1/2) endonuclease complex plays a crucial role in coordinating V(D)J recombination by introducing DNA breaks in immunoglobulin (*Ig*) loci. Dysregulation of RAG1/2 has been linked to the onset of B cell malignancies, yet the mechanisms controlling RAG1/2 in pre-B cells exposed to excessive DNA damage are not fully understood. In this study, we show that DNA damage–induced activation of p53 initiates a negative-feedback loop which rapidly downregulates RAG1 levels. This feedback loop involves ataxia telangiectasia mutated activation, subsequent stabilization of p53, and modulation of microRNA-34a (miR-34a) levels, which is one of the p53 targets. Notably, this loop incorporates transcription factor forkhead box P1 as a downstream effector. The absence of p53 resulted in an increased proportion of IgM$^+$ cells prompted to upregulate RAG1/2 and to undergo *Ig* light chain recombination. Similar results were obtained in primary pre-B cells with depleted levels of miR-34a. We propose that in pre-B cells undergoing *Ig* gene recombination, the DNA breaks activate a p53/miR-34a/forkhead box P1-mediated negative-feedback loop that contributes to the rapid downregulation of RAG. This regulation limits the RAG-dependent DNA damage, thereby protecting the stability of the genome during V(D)J rearrangement in developing B cells.

In developing pre-B cells, V(D)J rearrangement is orchestrated by the recombination activating gene 1 and 2 (RAG1/2) endonuclease complex. Aberrant regulation of this rearrangement process has been implicated in the development of B cell malignancies, such as B cell acute lymphoblastic leukemia (B-ALL) and follicular lymphoma (1–3). Persistent expression of RAG1 was shown to be an oncogenic driver in B-ALL (4) and RAG1/2 regulators have been suggested as plausible therapeutic targets (5–7). The double-stranded DNA breaks (DSBs) created by RAG1/2 activate the ataxia telangiectasia mutated (ATM) kinase, which then recruits and activates other proteins to the site of the breaks in the efforts of its repair (8). It has been shown that the DSBs themselves have a regulatory function and are able to modulate expression of other proteins and processes. For example, the RAG-dependent DSBs activate ATM, which was shown to limit RAG expression and accessibility of the *Igκ* locus, and thus enforcing allelic exclusion (9, 10). However, the mechanisms involved in DNA damage–induced modulation of RAG1/2 in developing pre-B cells are not entirely understood.

Previously, we have demonstrated that in response to external DNA damage, RAG protein and mRNA levels are rapidly downregulated and that the regulation involves the ATM-factor forkhead box O1 pathway, where pharmacological inhibition of ATM prevented the DNA damage–induced downregulation of *Rag1* and *Rag2*[6]. In the present study, we hypothesized that the DNA damage–induced regulation of *Rag1* and *Rag2* might involve p53 pathway. DNA damage–induced ATM activation has been shown to suppress the ubiquitin-mediated proteasomal degradation of p53, leading to its accumulation (11). Therefore, we investigated the involvement of downstream p53 targets in DNA damage–mediated regulation of *Rag1* and *Rag2*. MicroRNA-34a (miR-34a) is a known p53 downstream target which was demonstrated to modulate B cell development by affecting expression of RAG1/2 transcription factor forkhead box P1 (FOXP1) (12). Based on observations in our study, we propose that DNA damage regulates *Rag1* and *Rag2* expression through a feedback-loop involving p53/miR-34a/FOXP1.

Results and discussion

In line with our previous study (6), we further validated the involvement of ATM in the DNA damage–dependent regulation of RAG, and we expanded progenitor B cells from *Atm*$^{-/-}$ mouse bone marrows by interleukin-7 (IL7) and FMS-like tyrosine kinase 3 ligand (Flt3L) stimulation *in vitro*. The large-to-small pre-B cell transition was induced by IL7 and Flt3L withdrawal. In agreement with our previous findings, we show that IL7/Flt3L withdrawal induced *Rag1* and *Rag2* expression, which was downregulated upon 5 Gray (Gy) of γ-irradiation in

* For correspondence: Jeroen E. J. Guikema, J.E.Guikema@amsterdamumc.nl.

wildtype (WT) pre-B cells but not in $Atm^{-/-}$ pre-B cells (Fig. 1, *A*–*C*).

ATM activation is known to stabilize TP53 *via* a complex downstream array of events, including phosphorylation of mouse double minute 2, also known as E3 protein ubiquitin ligase, MDM2, which in its phosphorylated form cannot poly-ubiquitinate p53, thus leading to its stabilization (11, 13). Here, we show that the ATM-mediated regulation of *Rag* also involves p53. *Rag1* and *Rag2* mRNA was rapidly downregulated in response to external DNA damage in mouse primary pre-B cells, with on average 89.9% reduction in *Rag1* and 90.7% in *Rag2* mRNA levels in 5 Gy-irradiated primary WT pre-B cells, whereas in $Tp53^{-/-}$ mouse primary pre-B cells γ-irradiation resulted in an on average 44.3% reduction in *Rag1* and 25.6% in *Rag2* mRNA levels (Fig. 1, *D* and *E*). In addition, in one experiment in primary bone marrow pre-B cells prompted to undergo *Ig* light chain (Igl) recombination by IL7 and Flt3L withdrawal from the culture, the amount of surface IgM-expressing immature B cells ($B220^+DX6^-Ly6C\text{-}IgM^+$) was higher in $Tp53^{-/-}$ cultures cells as compared to their WT counterparts (1.32% *versus* 0.79%, respectively, Fig. S1*A*). Though not definitive, this result is consistent with the observed effect of p53 deficiency on *Rag1* and *Rag2* mRNA expression. As previously shown, p53 interferes with normal B cell development. For instance, sustained p53 activation as a consequence of wild-type p53-induced phosphatase 1 (*Wip1*) deficiency resulted in lower levels of $B220^{mid}CD43^-IgM^+CD19^+$ immature B cells in mice (14). However, it remains to be established if the p53-mediated decrease in *Rag1* and *Rag2* mRNA expression results in decreased expression of surface IgM in developing B cells and/or whether the effect of p53 (de)activation on B-cell development can be attributed to p53's ability to modulate apoptosis.

The transcription factor FOXP1 was shown to regulate RAG1 and RAG2 expression by binding to the *Erag* enhancer. The bone marrow from $Foxp1^{-/-}$ mice showed impaired B cell development, as the percentages of pro-B cells ($IgM^-B220^+CD43^+$) and pre-B cells ($IgM^-B220^+CD43^-$) were significantly lower than in $Foxp1^{+/-}$ bone marrows (15). In our study, the mRNA expression of *Foxp1* was decreased by 45.5% in γ-irradiated WT primary pre-B cell cultures undergoing light chain recombination following IL7 withdrawal, while the *Foxp1* expression in $Tp53^{-/-}$ primary pre-B cells remained unaffected by irradiation (Fig. 1*F*).

In the mouse A70 pre-B cell line, v-Abl creates a developmental block, arresting the B cells in a stage at which the RAG1/2 expression is low, and the *Igκ* is not yet recombined. Treatment with STI571, an Abelson-kinase inhibitor, alleviates this block and induces RAG1/2 expression and *Igκ* recombination (16). In agreement, in STI571-treated mouse v-Abl-transformed pre-B cells, 5 Gy γ-irradiation or treatment with the p53-stabilizing agent Nutlin-3 resulted in the downregulation of RAG1 and FOXP1 protein expression, which was prevented by pretreatment with the ATM kinase inhibitor KU55933 (Fig. 1*G*). The downregulation of RAG1 and FOXP1 following γ-irradiation was not caused by activation of caspases, as shown by pretreatment with the pan-caspase inhibitor Z-VAD-FMK, nor by cell death, as shown by the amount of sub-G1 phase cells analyzed by fluorescence-activated cell sorting (FACS) for DNA-content (propidium iodide). (Fig. S2, *A* and *B*).

Previously, we have shown that endogenous DNA damage emanating from RAG1/2 activity could trigger a similar regulatory response as provoked by γ-irradiation (6). To study the effect of RAG1/2-dependent DNA damage on *Foxp1* expression, we made use of pre-B cell cultures from $Rag1^{-/-}$ mice, where the developmental block imposed by *Rag1* deficiency is rescued by the transgenic expression of a functionally rearranged VH81x IgH μ chain (17). We observed that in *in vitro* cultured primary bone marrow B cell progenitor cells prompted to undergo *Igl* recombination by IL7 and Flt3L withdrawal, *Foxp1* mRNA levels were approximately 2-fold higher in $Rag1^{-/-}$ VH81x primary bone marrow as compared to their RAG-proficient counterparts (1.61-fold higher *Foxp1* levels, $p < 0.05$, on day 1 following IL7/Flt3L withdrawal in $Rag1^{-/-}$ VH81x *versus* $Rag1^{+/+}$ VH81x and 1.59-fold higher *Foxp1* levels, $p < 0.05$, on day 3 after IL7/Flt3L withdrawal in $Rag1^{-/-}$ VH81x *versus* $Rag1^{+/+}$ VH81x) (Fig. 1, *H* and *I*).

To further substantiate the role of FOXP1 in driving RAG expression in pre-B cells, we overexpressed the full-length (FL) FOXP1 and its shorter isoform (iso), which were previously shown to have similar functions (18), in the A70 v-Abl transformed mouse pre-B cell line (Fig. 2*A*). Interestingly, FOXP1 overexpression was sufficient to induce productive recombination *Igκ* recombination and partly overcame the development block imposed by v-Abl expression, as determined by the detection of productive by Vκ6-23-Jκ1 coding joints by polymerase chain reaction (PCR) (Fig. 2*B*). The FOXP1 isoform, truncated at the N terminus, is overexpressed in subsets of B cells lymphomas and has been suggested to have an oncogenic capacity (18–20). Our results imply that the FOXP1 N terminus is not required to partially override the v-Abl-induced developmental block in the A70 pre-B cell line. In addition, overexpression of BCL6 (21) a negative regulator of p53, also resulted in Vκ6-23-Jκ1 recombination events without STI571 treatment in A70 cells (Figs. 2, *A* and *B*, and S3, *A* and *B*). Similar to FOXP1-induced Vκ6-23-Jκ1 recombination event, also the B cell lymphoma 6 (BCL6)-induced Vκ6-23-Jκ1 recombination events occur at lower rates that the recombination events resulting from STI571 treatment, suggesting that BCL6 overexpression only partially overcame the developmental block imposed by v-Abl.

Previously, the regulation of FOXP1 in developing B cells was linked to the p53 pathway through miR-34a. The activation of p53 has been shown to drive the expression of miR-34a in cell lines of various origin (22–24), and constitutive miR-34a expression resulted in a B cell development blockade, where FOXP1 was identified as the key mediator of this effect (25). Moreover, in chronic lymphocytic leukemia cells, the p53/miR-34a pathway has been shown to be a negative regulator of FOXP1 expression, responding rapidly to DNA damage and limiting B cell receptor signaling in mature B cells (12). We therefore investigated the possible ties of ATM/p53 signaling induced by DSBs to the miR-34a/FOXP1/RAG axis. Our data show that γ-irradiation drives the miR-34a expression in *in vitro* expanded progenitor B cells from primary mouse bone marrow in a dose-dependent manner. In agreement, the level

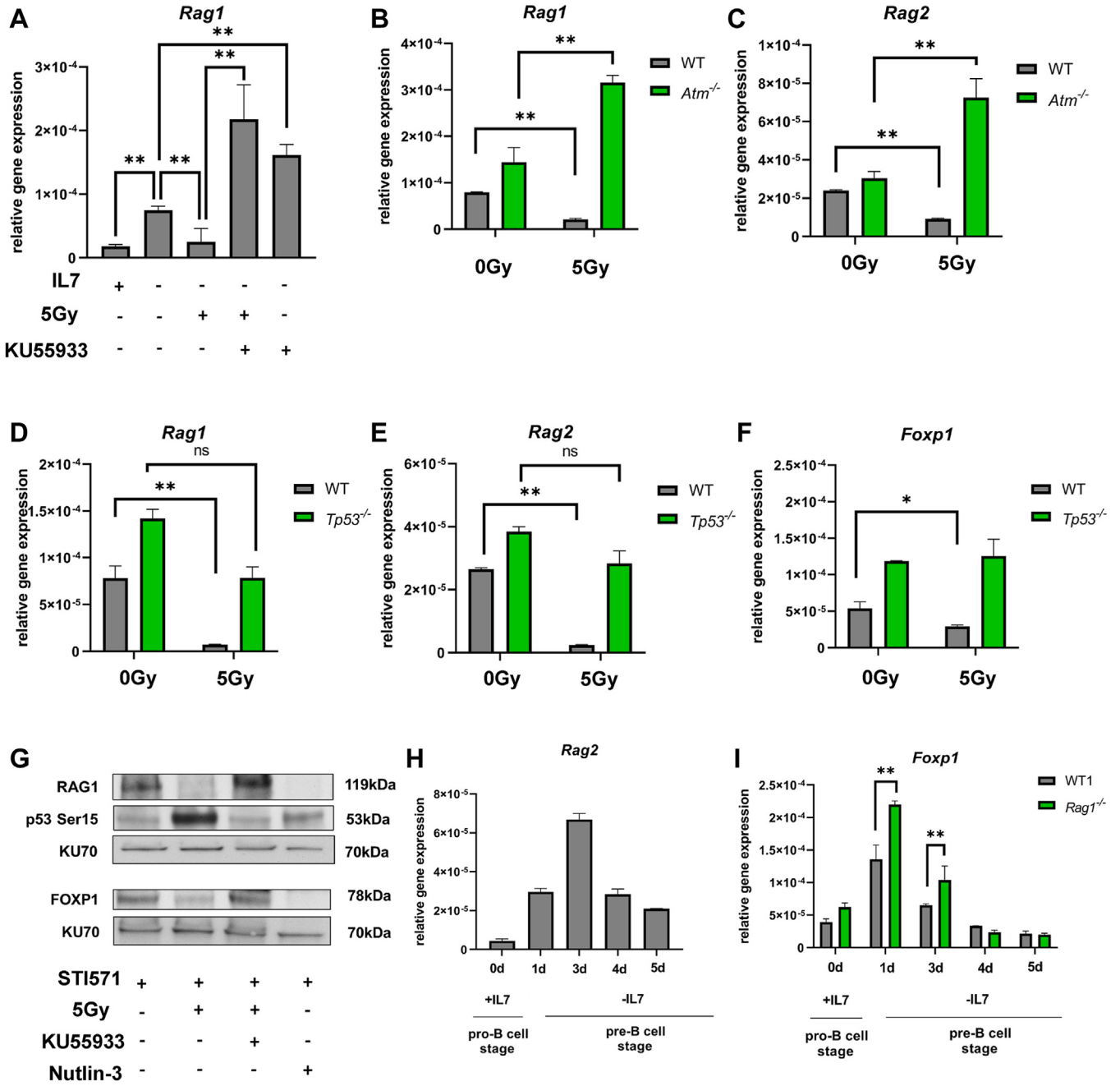

Figure 1. DNA damage-induced downregulation of *Rag1* and *Rag2* involves ATM and p53. *A*, *Rag1* mRNA expression in primary murine WT bone marrow pre-B cells measured by quantitative RT-PCR; the cells were first cultured 7 days on the OP9 feeder layer cell line with IL7 and Flt3L: conditions that promote expansion of small pre-B cells that have not yet undergone the *Igκ* recombination because of the low RAG1/2 expression. To induce the RAG1/2 expression, IL7 and Flt3L were withdrawn from the media for 24 h. After that, the cells were treated either with DMSO, subjected to 5 Gy γ-irradiation with subsequent 2 h recovery time, pretreated with ATM inhibitor KU55933 for 2 h prior to γ-irradiation, or treated for 4 h with KU55933 with no irradiation (n = 2, mean ± SD, $^{**}p < 0.05$). *B* and *C*, *Rag1* (*B*) and *Rag2* (*C*) mRNA expression in primary WT and $Atm^{-/-}$ bone marrow pre-B cells first cultured 7 days on OP9 cells with addition of IL7 and Flt3L, and 24 h after the withdrawal of Flt3L and IL7, the cells were treated either with either DMSO or subjected to 5 Gy γ-irradiation with subsequent 2 h recovery time (n = 2, mean ± SD, $^{**}p < 0.05$). *D* and *E*, *Rag1* and *Rag2* mRNA expression in primary WT and $Tp53^{-/-}$ bone marrow pre-B cells treated, 24 h after the withdrawal of Flt3L and IL7, with either DMSO or 5 Gy γ-irradiation with subsequent 2 h recovery time (n = 2, mean ± SD, fold difference as compared to DMSO, $^{*}p < 0.1$). *F*, *Foxp1* mRNA expression in primary WT and $Tp53^{-/-}$ bone marrow pre-B cells treated, 24 h after the withdrawal of Flt3L and IL7, with either DMSO or 5 Gy γ-irradiation with subsequent 2 h recovery time (n = 2, mean ± SD, fold difference as compared to DMSO, $^{*}p < 0.1$). *G*, Western blotting analysis of RAG1, TP53 phosphorylated at Ser[15], and FOXP1 protein levels in BV173 cells. The cells were treated with v-Abl kinase inhibitor STI571 for 72 h to induce RAG1/2 expression and *Igκ* recombination, after which the cells were exposed to 5 Gy γ-irradiation with subsequent 2 h recovery time or pretreated with ATM inhibitor KU55933 for 2 h prior to the irradiation with subsequent 2 h recovery time or treated with p53 stabilizer Nutlin-3 for 4 h. KU70 was used as a control. *H* and *I*, *Rag2* (*H*) and *Foxp1* (*I*) mRNA expression in primary WT and $Rag1^{-/-}$ bone marrow pre-B cells. After 7 days of culture, the Flt3L and IL7 were withdrawn from the media, and the *Rag2* and *Foxp1* mRNA expression were measured on the day of the withdrawal and 1, 3, 4, and 5 days following the withdrawal (n = 2, mean ± SD, $^{**}p < 0.05$). ATM, ataxia telangiectasia mutated; FOXP1, forkhead box P1; RAG1/2, recombination activating gene 1 and 2.

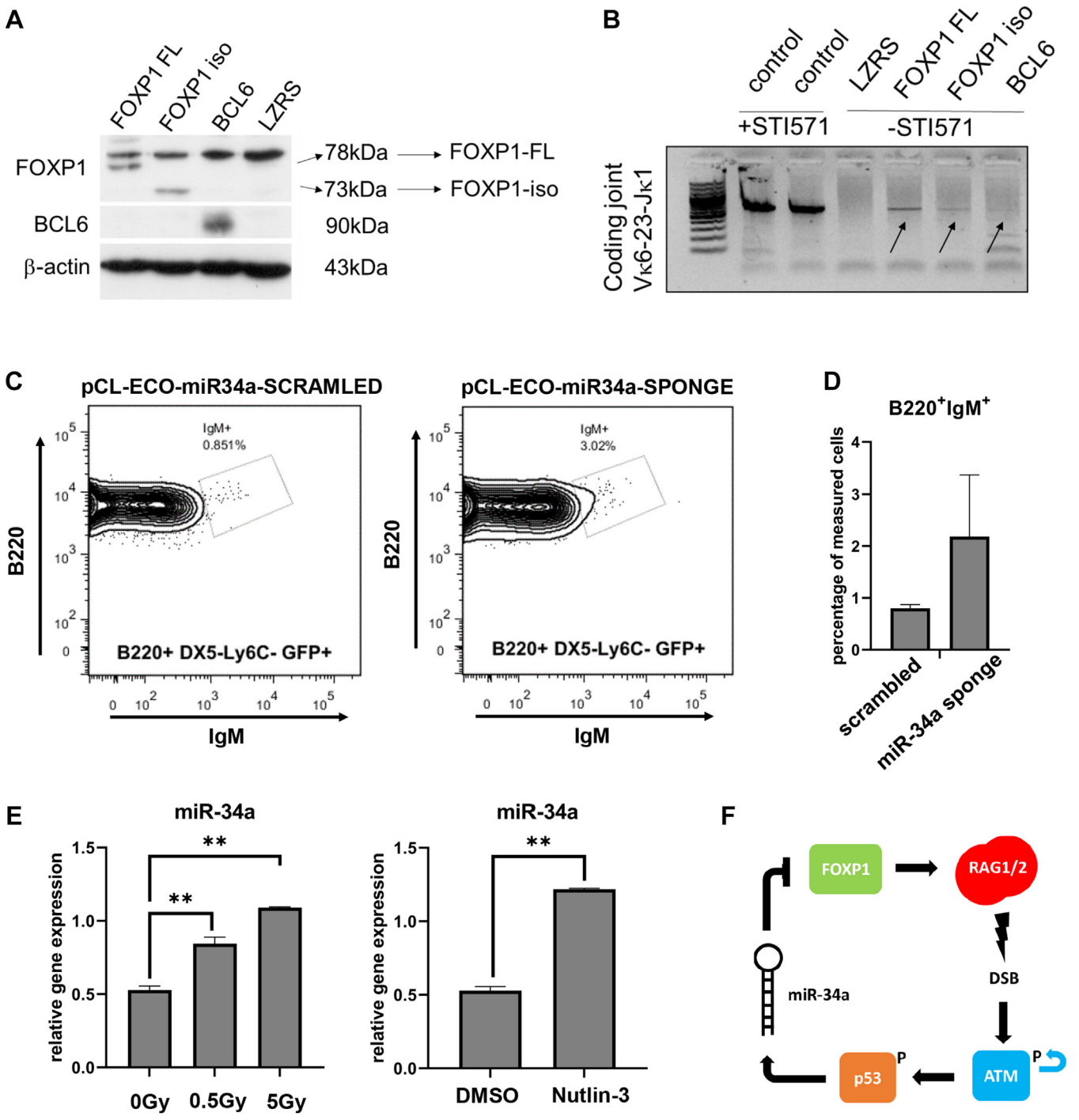

Figure 2. The DNA damage-induced miR-34a and its target FOXP1 regulate immunoglobulin light chain recombination in mouse pre-B cells. *A*, Western blotting analysis of FOXP1, BCL6, and β-actin (loading control) in mouse v-Abl WT (A70) cells transduced with either empty vector (LZRS), human full-length FOXP1 (FOXP1 FL), the isoform of human of FOXP1 (FOXP1 iso), or human BCL6. *B*, the mouse v-Abl WT cells (A70) were transduced with either empty vector (LZRS), human full-length FOXP1 (FOXP1 FL), the isoform of human of FOXP1 (FOXP1 iso), or human BCL6. Control, untransduced A70 cells treated with STI571 for 72 h to induce RAG1/2 expression and *Igκ* recombination. The formation of coding joints following the treatment with STI571 was assessed by qualitative PCR analysis of one particular joint: Vκ6-23 to *Jκ1* (31) (bands representing coding joints in transduced cells are indicated by *arrows*). The PCR products were run in 2% agarose gel containing ethidium bromide. *C*, representative FACS staining of WT primary bone marrow cells, transduced either with pCL-ECO-miR-34a-sponge or with pCL-ECO-scrambled as a control. The cells were cultured for 7 days on OP9, Flt3L, and IL7, the amount of $B220^{+}IgM^{+}$ pre-B cells was measured 48 h following the withdrawal of Flt3L and IL7 from the medium. *D*, quantification of the amount of $B220^{+}IgM^{+}$ pre-B cells by FACS staining as described in 2B (n = 2, mean ± SD, $^{**}p < 0.05$). *E*, RT-PCR analysis of the relative miR-34a expression in primary WT bone marrow pre-B cells, initially cultured 7 days on OP9, Flt3L, and IL7, then the Flt3L and IL7 were withdrawn from the medium for 72 h, and the cells were exposed to either 5 Gy or 0.5 Gy of γ-irradiation followed by 2 h of recovery or treated with p53 stabilizer Nutlin-3 (2.5 μM) for 4 h. Control cells were treated with DMSO (n = 2, mean ± SD, $^{**}p < 0.05$). *F*, schematic representation of the proposed self-regulating negative feedback loop. In response to excessive DNA damage ATM is phosphorylated which in turn activates the p53 pathway. Subsequently, one of the consequences of p53 activation of miR-34a, which is a negative regulator of FOXP1, the RAG1/2 transcription factor. This might represent a mechanism by which the B cells protect themselves against excessive DNA damage, and dysregulation of this pathway might contribute to the genetic instability in developing B cells. ATM, ataxia telangiectasia mutated; DSB, double-stranded DNA break; FOXP1, forkhead box P1; miR-34a, microRNA-34a; RAG1/2, recombination activating gene 1 and 2.

of miR-34a was significantly higher upon treatment with the MDM2 inhibitor Nutlin-3 (Fig. 2*E*). Furthermore, in *in vitro*-expanded progenitor B cells from primary bone marrow, depletion of miR-34a using a miR-34a-sponge construct resulted in an increase in $B220^+DX6^-Ly6C^-IgM^+$ B cells (2.19% in cells transduced with pCL-ECO-miR-34a-sponge *versus* 0.80% in cells transduced with pCL-ECO-scrambled) following the IL-7 and Flt3L withdrawal from the cell culture, suggesting that depletion of miR-34a promotes successful *Igκ* recombination (Fig. 2, *C* and *D*). As miR-34a has many targets, leaving the possibility that the stimulatory effect miR-34a depletion on B cell development might, partially, be carried out by other miR-34a target than FOXP1. Though the indirect nature of the evidence, the presented data are consistent with the proposed regulatory mechanism.

In summary, we propose a negative-feedback regulatory mechanism involving p53, miR-34a, and FOXP1, where DNA breaks limit the expression of RAG1 and RAG2 (Fig. 2*F*). In this regulatory mechanism, (RAG-dependent) DNA damage activates ATM, which in turn stabilizes p53 and activates the p53 effectors, including miR-34a, which affects FOXP1 levels and *Igκ* recombination in pre-B cells. In agreement, the levels of miR-34a as well as FOXP1 respond to exogenous and RAG-instigated DNA damage and limit the RAG1/2 expression and the V(D)J recombination. Our data are consistent with such a model, though further research is needed to describe its role conclusively. We suggest that this regulatory mechanism in developing B cells may serve as a self-protective mechanism against excessive RAG-dependent DNA damage and thus guards the stability of the genome.

Experimental procedures

Cell lines

Mouse and human v-Abl cells

The v-Abl transformed mouse pre–B cell lines were generated from WT (A70) and *Rag2*$^{-/-}$ (R2K3) mice that harbor the Eμ-Bcl2 transgene and were kindly provided by Dr Craig Bassing (University of Pennsylvania School of Medicine). The cells were cultured in RPMI1640 (Life Technologies) supplemented with 2 mM of L-glutamine, 100 U/ml penicillin, 100 μg/ml streptomycin, and 10% fetal calf serum (FCS) (Thermo Scientific) and 50 μM 2-mercaptoethanol (Sigma Aldrich). The human B cell receptor-ABL+ B-ALL cell line BV173 was obtained from the Deutsche Sammlung von Mikroorganismen und Zellkulturen (DSMZ) and cultured in RPMI1640 (Life Technologies) supplemented with 2 mM of l-glutamine, 100 U/ml penicillin, 100 μg/ml streptomycin, and 20% FCS. The following small-molecule inhibitors/activators were used: STI571 (imatinib methanesulfonate; LC Laboratories) to induce RAG1/2 expression in v-Abl cells and *Igl* recombination, the cells were treated with 5 μM STI571 as previously established (16, 26). KU55933 (ATM kinase inhibitor; Selleckchem), Nutlin-3 (nongenotoxic p53 activator (27), Sigma Aldrich), Z-VAD-FMK (carbobenzoxy-valyl-alanyl-aspartyl-[O-methyl]-fluoromethyl ketone; a pan-caspase inhibitor) (Promega), and Staurosporine (inductor of apoptosis through caspase-activation (28)) (Selleckchem).

Mouse primary B cells

ATM-deficient mice (29) (Jackson Laboratory stock 002753) and TP53-deficient mice (30) were provided by Dr Stephen Jones (University of Massachusetts Medical School). RAG1-deficient VH81x IgH μ chain transgenic mice were provided by Prof. Dr Rudi Hendriks (Erasmus Medical Center), and C57BL/6 WT mice were housed in the animal research facility of the Academic Medical Center under specific pathogen-free conditions. Animal experiments were approved by the Animal Ethics Committee (Dierenexperimentencommissie) and performed in agreement with national and institutional guidelines. Bone marrow cells were harvested from 8- to 20-weeks-old mice by flushing femurs and tibia. Total bone marrow cells were cultured in 6-well plates in RPMI1640 with 2 mM of L-glutamine, 100 U/ml penicillin, 100 μg/ml streptomycin, 10% FCS, 50 μM 2-mercaptoethanol, 10 ng/ml recombinant mouse IL-7, and 10 ng/ml Flt3L (both from ProSpec). The culture medium and cytokines were replaced every 3 days. Cells were harvested after 7 to 10 days and analyzed by flow cytometry, typically yielding >95% $B220^+IgM^-$ progenitor cells (Fig. S1*B*). To induce large to small pre–B cell transition, RAG1/2 expression, and *Igκ* recombination, the cells were washed three times in culture medium without cytokines and placed back in 6-well plates at 2×10^6 cells/ml in medium without cytokines (IL-7 withdrawal) (Fig. S1*C*).

The formation of coding joints was assessed by qualitative PCR analysis of Vκ6-23 to *Jκ1* rearrangement using previously published primers (31). The PCR products were separated in 2% agarose gel containing ethidium bromide.

Exogenous DNA damage and p53 induction

DNA damage was induced by irradiating the cells ([^{137}Cs], 5 Gy, 0.50 Gy/min) at a dose of 5 Gy. In some experiments, dose dependency was studied, in these cases, where indicated so, also a 0.5 Gy dose was applied. After γ-irradiation, the cells were allowed to recover for 2 h at 37 °C in an atmosphere of 5% CO2 and subsequently harvested. To study the effect on p53 activation without the genotoxic element, the cells were treated with Nutlin-3 by adding 2.5 μM of the compound into the cell culture, and after 2 h, the cells were thoroughly washed and collected.

Western blot

The protein pellets were homogenized passing through a 27G needle, and protein concentrations were measured using the bicinchoninic acid assay (Sigma-Aldrich). For each sample, 15 μg of protein lysate was used for protein separation in Precise 4 to 20% gradient Tris-SDS gels (Thermo Fisher Scientific). Subsequently, separated protein lysates were transferred onto polyvinylidene difluoride membranes (Immobilon-P; EMD Millipore); membranes were blocked in 5% BSA (BSA Fraction V, Roche Life Sciences) in TBS-T or 5% milk in TBS-T for 2 h. Primary antibodies (Abs) were incubated overnight at 4 °C. After a series of thorough washes with TBS-T, membranes were incubated with secondary Abs (goat anti-rabbit HRP or rabbit anti-mouse HRP; DAKO, Agilent

Technologies) for 2 h at room temperature. Ab binding (protein expression) was visualized using Amersham ECL Prime Western blotting detection reagent (GE Healthcare Bio-Sciences AB). The blots were quantified visually. The following Abs were used in this study: rabbit anti-RAG1 (D36B3), rabbit anti-FOXP1, rabbit anti–phospho-p53 Ser^{15}) (9284), rabbit anti-cleaved caspase-3 (Asp^{175}) (9661), rabbit anti-BCL6, rabbit anti- KU70 (D10A7), all from Cell Signaling Technology, rabbit anti-FOXP1 ab16645 (Abcam), and mouse anti–β-actin (C4) (EMD Millipore).

Real-time quantitative PCR

The RNA isolation from the cells was performed using TRIreagent (Sigma-Aldrich) according to the manufacturer's protocol. MicroRNA isolation was performed using mirVana miRNA isolation kit (ThermoFisher) according to the manufacturer's protocol.

Levels of mRNA expression were determined using the CFX384 (Bio-Rad) real-time PCR platform. For each sample, cDNA was synthesized from 500 ng of RNA, using random primers (Promega) and Moloney murine leukemia virus reverse transcriptase (Invitrogen-Life Technologies). For each sample, cDNA was diluted 1:5 with PCR-grade water. The PCR master mix contained 5 μl of Sso Fast EvaGreen supermix (Bio-Rad) and 0.5 μl of 10 μM reverse and forward primers (Biolegio). The final volume was adjusted to 9 μl using PCR-grade water to which 1 μl of diluted cDNA was added. The following PCR conditions were used: initial denaturation at 95 °C for 5 min, followed by 40 cycles of denaturation at 95 °C for 15 s, annealing at 65 °C for 5 s, and extension at 72 °C for 10 s. The fluorescent product was measured by a single acquisition mode at 72 °C after each cycle. For distinguishing specific from nonspecific products and primer dimers, a melting curve was obtained after amplification by holding the temperature at 65 °C for 15 s followed by a gradual increase in temperature to 95 °C at a rate of 2.5 °C s^{-1}, with the signal acquisition mode set to continuous. For each cDNA preparation, PCRs were performed at least in duplicate, and for each condition, at least three independent experiments were performed. Expression of target gene mRNAs was normalized to the housekeeping genes large ribosomal protein PO (*RPLPO*) for human samples and 18S rRNA (*18S rRNA*) for mouse samples. Expression of miR-34a was assessed by Taqman MicroRNA assay and normalized to snoRNA429 (Applied; now ThermoFisher) as per manufacturer's protocol.

The following primers were used: mouse Rag1-forward (5′-AGCTATCACTGGGAGGCAGA-3′), mouse Rag1-reverse (5′-GAGGAGGCAAGTCCAGACAG-3′), mouse Rag2-forward (5′-CTTCCCCAAGTGCTGACAAT-3′), mouse Rag2-reverse (5′-AGTGAGAAGCCTGGCTGAAT-3′), mouse Foxp1-forward (5′-AGTCATGATGCAAGAATCTGGGT-3′), mouse Foxp1-reverse (5′- TCTCCGTTGGACCGAGTGT-CACG-3′) mouse 18S rRNA-forward (5′-TGGTGGAGG-GATTTGTCTGG-3′), and mouse 18S rRNA-reverse (5′-TCAATCTCGGGTGGCTGAAC-3′). The data were analyzed in GraphPad, on figures expressed as mean ± SD, and one-way ANOVA statistical analysis with Sidak *post hoc* test was used for multiple comparisons with the alpha threshold of 0.05. Where data are compared as fold induction/reduction against a control group, a nonparametric Kruskal–Wallis test with Dunn's *post hoc* test was used with the alpha threshold set to 0.1 due to a low number of repeats.

FACS

Flow-cytometry staining and analyses were performed according to the protocol as described earlier (5). Briefly, 1 × 10^6 cells were washed 2× with 2 ml of cold FACS buffer (1x PBS + 0. 2% NaN3 + 1% FCS) and spun at 1100 rpm for 5 min. After the addition of the Abs, the cells were incubated on ice in the dark for 30 min and then washed again with the cold FACS buffer. Next, the cells were resuspended in 1 ml 1× PBS + 1% paraformaldehyde and incubated for 5 min at room temperature. Finally, the cells were spun at 1100 rpm and resuspended again in 400 μl of FACS buffer. The doublets were excluded based on forward and side scatter height *versus* width profiles. Flow cytometry was performed on a four-laser, thirteen-detector LSR Fortessa (BD Biosciences). Flow cytometry data were analyzed using FlowJo (Tree Star Inc). The following Abs were used to perform the stainings: rat-anti-mouse CD45R/B220 (BD Pharmingen, clone RA3-682) rat-anti-mouse CD43 (BD Pharmingen, clone S7), rat-anti-mouse Ig kappa light chain (BD Pharmingen, clone 187.1), rat anti-mouse IgM (eBioscience, clone II/41), rat-anti-mouse IgD (Southern Biotech, clone 11-26), rat-anti-mouse CD49b (BD Pharmingen, clone DX5), and rat-anti-mouse Ly-6C (BD Pharmingen, clone AL-21).

Retroviral transductions

LZRS-FOXP1-IRES-YFP (FOXP1 FL) and LZRS-BCL6-IRES-GFP (BCL6) were generated as previously described (18, 21). A FOXP1-iso construct that starts translation from the second coding ATG (in exon 6; M101), encoding a 100 AA N terminally deleted FOXP1, was PCR-cloned and subcloned into LZRS-IRES-YFP (FOXP1 iso). Cells transduced with an empty LZRS-IRES-YFP were used as a control.

The pCL-ECO-miR-34a-sponge and pCL-ECO-scrambled were kindly provided by Dr J. Kluiver, University Medical Center Groningen, The Netherlands. The viral transductions were performed as previously described (18, 21, 32). Transduced cells were FACS-sorted based on GFP expression 5 days after transduction.

Data availability

The data that support the findings of this study are available from the corresponding author, Dr J. E. J. Guikema, upon reasonable request.

Supporting information—This article contains supporting information.

Author contribution—K. O.-M., M. v. K., M. S., C. J. M. v. N., and J. E. J. G. writing–review & editing; K. O.-M. and J. E. J. G. writing–

original draft; K. O.-M. and M. v. K investigation; K. O.-M., M. v. K., and J. E. J. G. formal analysis; K. O.-M., M. S., C. J. M. v. N., and J. E. J. G. data curation; K. O.-M., M. S., C. J. M. v. N., and J. E. J. G. conceptualization; M. v. K. and C. J. M. v. N. methodology; M. S. resources; J. E. J. G. supervision; J. E. J. G. project administration; J. E. J. G. funding acquisition.

Funding and additional information—This study was supported by the Academic Medical Center Fellowship program and a VIDI-grant from the Dutch Organization for Scientific Research (NWO VIDI 016126355), both awarded to J. E. J. G.

Conflict of interest—The authors declare no conflict of interest with the contents of this article.

Abbreviations—The abbreviations used are: ATM, ataxia telangiectasia mutated; B-ALL, B cell acute lymphoblastic leukemia; DSB, double-stranded DNA break; FOXP1, forkhead box P1; *Ig*, immunoglobulin; Igl, Ig light chain; miR-34a, microRNA-34a; RAG1/2, recombination activating gene 1 and 2; WT, wildtype.

References

1. Bakhshi, A., Wright, J. J., Graninger, W., Seto, M., Owens, J., Cossman, J., *et al.* (1987) Mechanism of the t(14;18) chromosomal translocation: structural analysis of both derivative 14 and 18 reciprocal partners. *Proc. Natl. Acad. Sci. U. S. A.* **84**, 2396–2400
2. Kuiper, R. P., and Waanders, E. (2014) A RAG driver on the road to pediatric ALL. *Nat. Genet.* **46**, 96–98
3. Papaemmanuil, E., Rapado, I., Li, Y., Potter, N. E., Wedge, D. C., Tubio, J., *et al.* (2014) RAG-mediated recombination is the predominant driver of oncogenic rearrangement in ETV6-RUNX1 acute lymphoblastic leukemia. *Nat. Genet.* **46**, 116–125
4. Han, Q., Ma, J., Gu, Y., Song, H., Kapadia, M., Kawasawa, Y. I., *et al.* (2019) RAG1 high expression associated with IKZF1 dysfunction in adult B-cell acute lymphoblastic leukemia. *J. Cancer* **10**, 3842–3850
5. Ochodnicka-Mackovicova, K., Bahjat, M., Bloedjes, T. A., Maas, C., de Bruin, A. M., Bende, R. J., *et al.* (2015) NF-κB and AKT signaling prevent DNA damage in transformed pre-B cells by suppressing RAG1/2 expression and activity. *Blood* **126**, 1324–1335
6. Ochodnicka-Mackovicova, K., Bahjat, M., Maas, C., van der Veen, A., Bloedjes, T. A., de Bruin, A. M., *et al.* (2016) The DNA damage response regulates RAG1/2 expression in pre-B cells through ATM-FOXO1 signaling. *J. Immunol.* **197**, 2918–2929
7. Wang, F., Demir, S., Gehringer, F., Osswald, C. D., Seyfried, F., Enzenmüller, S., *et al.* (2018) Tight regulation of FOXO1 is essential for maintenance of B-cell precursor acute lymphoblastic leukemia. *Blood* **131**, 2929–2942
8. Maréchal, A., and Zou, L. (2013) DNA damage sensing by the ATM and ATR kinases. *Cold Spring Harb. Perspect. Biol.* **5**, a012716
9. Glynn, R. A., and Bassing, C. H. (2022) Nemo-dependent, ATM-mediated signals from RAG DNA breaks at Igk feedback inhibit V (κ) recombination to enforce Igκ allelic exclusion. *J. Immunol.* **208**, 371–383
10. Steinel, N. C., Lee, B. S., Tubbs, A. T., Bednarski, J. J., Schulte, E., Yang-Iott, K. S., *et al.* (2013) The ataxia telangiectasia mutated kinase controls Igκ allelic exclusion by inhibiting secondary Vκ-to-Jκ rearrangements. *J. Exp. Med.* **210**, 233–239
11. Cheng, Q., and Chen, J. (2010) Mechanism of p53 stabilization by ATM after DNA damage. *Cell Cycle Georget. Tex* **9**, 472–478
12. Cerna, K., Oppelt, J., Chochola, V., Musilova, K., Seda, V., Pavlasova, G., *et al.* (2019) MicroRNA miR-34a downregulates FOXP1 during DNA damage response to limit BCR signalling in chronic lymphocytic leukaemia B cells. *Leukemia* **33**, 403–414
13. Shiloh, Y., and Ziv, Y. (2013) The ATM protein kinase: regulating the cellular response to genotoxic stress, and more. *Nat. Rev. Mol. Cell Biol.* **14**, 197–210
14. Yi, W., Hu, X., Chen, Z., Liu, L., Tian, Y., Chen, H., *et al.* (2015) Phosphatase Wip1 controls antigen-independent B-cell development in a p53-dependent manner. *Blood* **126**, 620–628
15. Hu, H., Wang, B., Borde, M., Nardone, J., Maika, S., Allred, L., *et al.* (2006) Foxp1 is an essential transcriptional regulator of B cell development. *Nat. Immunol.* **7**, 819–826
16. Muljo, S. A., and Schlissel, M. S. (2003) A small molecule Abl kinase inhibitor induces differentiation of Abelson virus-transformed pre-B cell lines. *Nat. Immunol.* **4**, 31–37
17. Stadhouders, R., de Bruijn, M. J. W., Rother, M. B., Yuvaraj, S., Ribeiro de Almeida, C., Kolovos, P., *et al.* (2014) Pre-B cell receptor signaling induces immunoglobulin κ locus accessibility by functional redistribution of enhancer-mediated chromatin interactions. *PLoS Biol.* **12**, e1001791
18. van Keimpema, M., Grüneberg, L. J., Schilder-Tol, E. J. M., Oud, M. E. C. M., Beuling, E. A., Hensbergen, P. J., *et al.* (2017) The small FOXP1 isoform predominantly expressed in activated B cell-like diffuse large B-cell lymphoma and full-length FOXP1 exert similar oncogenic and transcriptional activity in human B cells. *Haematologica* **102**, 573–583
19. Brown, P. J., Ashe, S. L., Leich, E., Burek, C., Barrans, S., Fenton, J. A., *et al.* (2008) Potentially oncogenic B-cell activation-induced smaller isoforms of FOXP1 are highly expressed in the activated B cell-like subtype of DLBCL. *Blood* **111**, 2816–2824
20. Green, M. R., Gandhi, M. K., Courtney, M. J., Marlton, P., and Griffiths, L. (2009) Relative abundance of full-length and truncated FOXP1 isoforms is associated with differential NFkappaB activity in Follicular Lymphoma. *Leuk. Res.* **33**, 1699–1702
21. van Keimpema, M., Grüneberg, L. J., Mokry, M., van Boxtel, R., van Zelm, M. C., Coffer, P., *et al.* (2015) The forkhead transcription factor FOXP1 represses human plasma cell differentiation. *Blood* **126**, 2098–2109
22. Chang, T.-C., Wentzel, E. A., Kent, O. A., Ramachandran, K., Mullendore, M., Lee, K. H., *et al.* (2007) Transactivation of miR-34a by p53 broadly influences gene expression and promotes apoptosis. *Mol. Cell* **26**, 745–752
23. Okada, N., Lin, C. P., Ribeiro, M. C., Biton, A., Lai, G., He, X., *et al.* (2014) A positive feedback between p53 and miR-34 miRNAs mediates tumor suppression. *Genes Dev.* **28**, 438–450
24. Navarro, F., and Lieberman, J. (2015) miR-34 and p53: new insights into a complex functional relationship. *PLoS One* **10**, e0132767
25. Rao, D. S., O'Connell, R. M., Chaudhuri, A. A., Garcia-Flores, Y., Geiger, T. L., and Baltimore, D. (2010) MicroRNA-34a perturbs B lymphocyte development by repressing the forkhead box transcription factor Foxp1. *Immunity* **33**, 48–59
26. Pegoraro, L., Matera, L., Ritz, J., Levis, A., Palumbo, A., and Biagini, G. (1983) Establishment of a Ph1-positive human cell line (BV173). *J. Natl. Cancer Inst.* **70**, 447–453
27. Shen, H., and Maki, C. G. (2011) Pharmacologic activation of p53 by small-molecule MDM2 antagonists. *Curr. Pharm. Des.* **17**, 560–568
28. Chae, H. J., Kang, J. S., Byun, J. O., Han, K. S., Kim, D. U., Oh, S. M., *et al.* (2000) Molecular mechanism of staurosporine-induced apoptosis in osteoblasts. *Pharmacol. Res.* **42**, 373–381
29. Barlow, C., Hirotsune, S., Paylor, R., Liyanage, M., Eckhaus, M., Collins, F., *et al.* (1996) Atm-deficient mice: a paradigm of ataxia telangiectasia. *Cell* **86**, 159–171
30. Donehower, L. A., Harvey, M., Slagle, B. L., McArthur, M. J., Montgomery, C. A., Butel, J. S., and Bradley, A. (1992) Mice deficient for p53 are developmentally normal but susceptible to spontaneous tumours. *Nature* **356**, 215–221
31. Bredemeyer, A. L., Sharma, G. G., Huang, C. Y., Helmink, B. A., Walker, L. M., Khor, K. C., *et al.* (2006) ATM stabilizes DNA double-strand-break complexes during V(D)J recombination. *Nature* **442**, 466–470
32. van Keimpema, M., Grüneberg, L. J., Mokry, M., van Boxtel, R., Koster, J., Coffer, P. J., *et al.* (2014) FOXP1 directly represses transcription of pro-apoptotic genes and cooperates with NF-κB to promote survival of human B cells. *Blood* **124**, 3431–3440